Correspondence

On Exploiting Sampling Jitter in Vehicular Sensor Networks

Baris Atakan

***Abstract*—Vehicular sensor networks (VSNs) are composed of vehicular sensor nodes that collaboratively sample, communicate, and reconstruct the event signal at the sink node. Samples of event signals are subjected to jitter based on the propagation speed of signal and locations of vehicular sensors. In this paper, a theoretical analysis is presented to understand the effects and how to exploit the jitter in the sensed event signal for energy-efficient and reliable communication in VSNs. Results reveal that sampling jitter can be advantageous and can be exploited in developing adaptive communication techniques, which can provide significant energy conservation while maintaining reliability in VSNs.**

***Index Terms*—Energy conservation, irregular sampling, sampling jitter, vehicular sensors.**

I. Introduction

Vehicular sensor networks (VSNs) consist of movable sensor nodes, i.e., vehicular sensors, that aim to efficiently communicate the sensed event signal to the sink. To satisfactorily reconstruct the event signal and to meet application objectives, a sufficient number of distinct samples needs to be taken and delivered to the sink node by vehicular sensors according to the Nyquist sampling theory [1]. In the existing literature, the reconstruction of the observed phenomenon in wireless sensor networks (WSNs) has been extensively researched [3]–[5]. In [6], the irregular spatiotemporal sampling is investigated to mitigate the irregularity of the sampling rather than exploiting it. In [7], the band-limited event signal reconstruction from the irregularly spaced samples is comprehensively investigated. Although these works can successfully investigate the irregular sampling phenomenon in WSNs, none of these works investigates sampling jitter in WSNs or VSNs. The main objective of this paper is to investigate the effects and potential advantages of sampling jitter to improve the performance of event signal reconstruction and energy conservation in VSNs. To this end, the event signal sampled by the sensor nodes[1] is first modeled, and a reconstruction scheme used by the sink node to reconstruct the event signal from its jittered samples is introduced. Then, an approach to exploit the sampling jitter is presented to improve the energy efficiency and reliability of sensor communication in VSNs. Through numerical analysis, it is shown that sampling jitter may indeed be exploited toward energy conservation and reliability.

Manuscript received December 12, 2011; revised February 11, 2013 and April 17, 2013; accepted May 30, 2013. Date of publication June 26, 2013; date of current version January 13, 2014. The review of this paper was coordinated by Prof. J.-M. Chung.

The author is with the Department of Electrical and Electronics Engineering, Izmir Institute of Technology, Izmir 35430, Turkey (e-mail: barisatakan@iyte.edu.tr).

Color versions of one or more of the figures in this paper are available online at http://ieeexplore.ieee.org.

Digital Object Identifier 10.1109/TVT.2013.2271359

[1]Throughout this paper, the terms sensor node and vehicular sensor node are interchangeably used to call the vehicular sensor nodes in VSNs.

The remainder of the paper is organized as follows. In Section II, two different schemes are proposed to exploit the sampling jitter to improve the energy efficiency in VSNs. The numerical results are given in Section III, and the concluding remarks are presented in Section IV.

II. Exploiting Sampling Jitter in Vehicular Sensor Networks

In VSNs or WSNs, an event is mostly assumed to be a point source that generates a signal called event signal, i.e., $h_S(t)$, at location $(0, 0)$. If the propagation velocity of $h_S(t)$ is v, sensor node i at location (x_i, y_i) receives the signal

$$h(x_i, y_i, t) = h_S\left(t - \frac{\sqrt{x_i^2 + y_i^2}}{v}\right) \tag{1}$$

where $h(x_i, y_i, t)$ can be also considered as a jittered version of event signal $h_S(t)$. In addition to the jitter due to the propagation speed of $h_S(t)$, the timing noise of sampling in the sensor processor also causes a jitter in the sample points taken by sensor nodes. However, this timing noise is considerably lower than the signal propagation delay. For example, for the Berkeley Mica Mote whose allowable sampling frequency is 200 Hz, this timing noise is considerably lower than 1/200 s. However, in a WSN monitoring some acoustic signals with the speed 340 m/s, the signal propagation delay is 0.059 s for two sensor nodes that are 20 m distant from each other. Hence, the timing noise of the sensor processor can be omitted.

Here, two different phases of sensor nodes are considered. In the first phase, which is called *immobile data gathering phase*, vehicular sensor nodes are assumed to stop whenever they detect an event signal; then, they sense and sample it without moving. In the other phase called *mobile data gathering phase*, sensor nodes are assumed to continuously move in the environment to gather the event information without stopping. Next, these two phases are separately detailed.

A. Exploiting Sampling Jitter in Immobile Data Gathering

Let us assume that sensor nodes detect an event signal and stop moving to sense and sample the event signal with the sampling frequency f (in Hertz). Hence, the set of the samples taken and transmitted to the sink node by sensor node i within a second, i.e., u_i, can be expressed as $u_i = \{h_S(t_0 - \tau_i), h_S(t_0 + (1/f) - \tau_i), h_S(t_0 + (2/f) - \tau_i), \ldots, h_S(t_0 + (f - 1/f) - \tau_i)\}$. Here, τ_i is the sampling jitter of sensor node i and is given as $\tau_i = \sqrt{x_i^2 + y_i^2}/v$. These sample sets $(u_i, \forall i)$ are assumed to be delivered to the sink node without any loss, and the sink node is assumed to superpose them to generate the irregularly sampled event signal, as shown in Fig. 1. Let us also suppose that m sensor nodes sample $h_S(t)$. Hence, the sink node receives $R = mf$ distinct samples within the interval $[t_0 - (1/f), t_0 - (1/f) + 1]$. Assume that the sampling points of these samples are given as $(t_0 - (1/f)) \leq n_0 < n_1 < \cdots < n_{R-1} \leq (t_0 - (1/f) + 1)$. The reconstruction of $h_S(t)$ from the irregularly spaced samples, i.e., $h_S(n_0), h_S(n_1), \ldots, h_S(n_{R-1})$, primarily requires the condition $R = mf \geq 2N + 1$ to be satisfied. This condition resembles the Nyquist rate condition required for the reconstruction

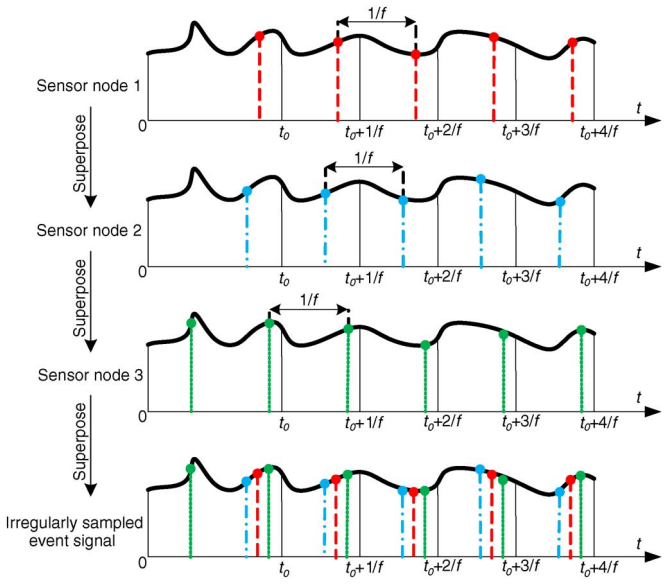

Fig. 1. Jittered samples are superposed to generate irregularly sampled signals.

of a uniformly sampled signal with bandwidth N. In addition to this, the condition $\zeta_i = n_{i-1} - n_i < (1/2N)$, $i \in \{1, \ldots, R-1\}$ on the timing gap between the consecutive sampling points can be sufficient to ensure an accurate reconstruction [7], [8]. Let us now concentrate on the sampling points at the interval $[t_0 - (1/f), t_0]$. The sample point of each sensor node i in this interval, i.e., g_i, can be also given as

$$g_i = \begin{cases} t_0 - \tau_i, & \text{if } \frac{1}{f} \geq \tau_i \\ t_0 - \tau_i + \frac{1}{f}\lfloor f\tau_i \rfloor, & \text{if } \frac{1}{f} < \tau_i \end{cases} \quad (2)$$

where $\lfloor \cdot \rfloor$ is the floor function. Let $\mathbf{g}$ be a vector including all sampling points of sensor nodes in the interval $[t_0 - (1/f), t_0]$, i.e., $\mathbf{g} = [g_1, g_2, \ldots, g_m]$. The sorted version of $\mathbf{g}$ can be also defined as $\widehat{\mathbf{g}} := \mathbf{sort}(\mathbf{g})$, where $\mathbf{sort}(\cdot)$ is a function that sorts the elements of a vector in increasing order and returns a sorted vector. The elements of $\widehat{\mathbf{g}}$ are the first m of the irregular sampling points $n_0, n_1, \ldots, n_{m-1}, \ldots, n_{R-1}$, i.e., $\widehat{\mathbf{g}} = [n_0, \ldots, n_{m-1}]$. In fact, the sample points follow a periodic pattern since each sensor node uses the sampling frequency f. This can be easily observed in Fig. 1.Hence, if the first m sampling points, i.e., $n_0, \ldots, n_{m-1}$, are known, the remaining sampling points can be easily generated by using $n_i = \widehat{\mathbf{g}}(\widetilde{i}) + (1/f)\lfloor i/m \rfloor$, for $m \leq i \leq R-1$, where $i \equiv \widetilde{i} \mod (m)$, or in other words, $\widetilde{i}$ is the remainder in the division of i by m. $\widehat{\mathbf{g}}(\widetilde{i})$ is the $\widetilde{i}$th element of the vector $\widehat{\mathbf{g}}$. Hence, by using the vector $\widehat{\mathbf{g}}$, it can be possible to deduce whether the condition $\zeta_i = n_{i-1} - n_i < (1/2N)$ is satisfied. In fact, ζ_i is always less than or equal to $1/f$, i.e., $\zeta_i \leq (1/f)$, since all sensor nodes sample the event signal with the sampling frequency f. Therefore, an appropriate sampling frequency f can be always found to ensure that $\zeta_i < (1/2N)\ \forall i$, which is needed for the accurate reconstruction of the event signal from the irregular samples. Hence, the selection of f is subjected to two conditions $R = mf \geq 2N + 1$ and $\zeta_i = n_{i-1} - n_i < (1/2N)$, $i \in \{1, \ldots, R-1\}$. By combining these conditions, the minimization of energy consumption can be formulated by

$$\begin{aligned} &\text{minimize} && f \\ &\text{subject to} && mf \geq 2N+1 \quad \text{and} \quad \zeta_i < \frac{1}{2N} \quad \forall i. \end{aligned} \quad (3)$$

Here, the sink node is assumed to know the locations of all vehicular sensor nodes and the event source[2]; thus, it can easily compute the distances from the vehicular sensors to the event source. Using this information and the propagation velocity of the event signal, the sink node can also calculate the sampling jitter and the timing gaps between consecutive sampling points, i.e., $\zeta_i\ \forall i$. Consequently, based on all of these information, the sink node can employ the following iterative procedure to solve the optimization problem formulated in (3) to find the minimum sampling frequency. Then, the sink sets it as the sampling frequency of sensor nodes.

1) Initially, set f as $f = (2N+1)/m$, which initially provides $mf = 2N + 1$.
2) Until $\zeta_i < (1/2N)$ is satisfied for all i, update f as $f = f + \delta$, where δ is a positive small constant. Note that, after initially setting f as $f = (2N+1)/m$ and iteratively increasing f with δ, the condition $mf \geq 2N + 1$ can be always satisfied.
3) If $\zeta_i < (1/2N)$ is satisfied for all i, set the last updated f as the minimum f.

The pseudocode for this procedure is given in Algorithm 1.

Algorithm 1: Immobile Data Gathering Phase

set f as $f = (2N+1)/m$
compute $\zeta_i = n_{i-1} - n_i\ \forall i \in \{1, \ldots, R-1\}$
while $\zeta_i > (1/2N)$ *for any* i **do**
$f = f + \delta$
compute $\zeta_i\ \forall i$ using the updated f
end
announce the last updated f as the sampling frequency

B. Exploiting Sampling Jitter in Mobile Data Gathering

In the mobile data gathering phase, the distance between each sensor node and the event source continuously changes due to the mobility of the sensor nodes. Therefore, the sampling jitter of each sensor node changes as its location alters with respect to the event source location. Due to this jitter, each sensor node i can take the samples during a second at different time points. The set including these time points, i.e., p_i, can be given as $p_i = \{\lambda_0 - J_i(\lambda_0), \lambda_1 - J_i(\lambda_1), \ldots, \lambda_{f-1} - J_i(\lambda_{f-1})\}$, where λ_k can be given as $\lambda_k = t_0 + (k/f)$, and $J_i(\lambda_k)$ is the jitter experienced by sensor node i at time λ_k and can be given as $J_i(\lambda_k) = \sqrt{x_i(\lambda_k)^2 + y_i(\lambda_k)^2}/v$, with v being the propagation speed of $h_S(t)$, and $[x_i(\lambda_k), y_i(\lambda_k)]$ representing the coordinate of the sensor i location at time λ_k. Note that each sensor node i is assumed to send its location information l_i to the sink node at the time, i.e., $l_i = \{[x_i(\lambda_1), y_i(\lambda_1)], \ldots, [x_i(\lambda_f), y_i(\lambda_f)]\}$. Based on the location information, $l_i \forall i$, the sink node computes the sampling jitter for all sensor nodes, i.e., $J_i(\cdot)\ \forall i$. Then, it can compute the sample points, i.e., $p_i\ \forall i$. Let $\mathbf{y}$ be a vector including all sampling points of m sensor nodes, i.e., $\mathbf{y} = [p_1, p_2, \ldots, p_m]$. The sorted version of $\mathbf{y}$ can be also defined by $\widehat{\mathbf{y}} = \mathbf{sort}(\mathbf{y})$. The elements of $\widehat{\mathbf{y}}$ are the irregular sampling points, $k_0, k_1, \ldots, k_{mf}$, i.e., $\widehat{\mathbf{y}} = [k_0, \ldots, k_{mf-1}]$, where m and f represent the number of sensor nodes and the sampling frequency, respectively.

[2]The event source localization and node localization are beyond the scope of this paper. However, in the literature, there is an extensive set of research works on these localization techniques. More specifically, various event source localization techniques can be reviewed in [9]. Similarly, common node localization techniques devised for WSNs can be found in [10].

Using $\widehat{\mathbf{y}}$, the sink node can also find the timing gap between the consecutive samples, i.e., η_i, as $\eta_i = (k_i - k_{i-1})$, $i \in \{1, \ldots, mf - 1\}$. As introduced in the immobile data gathering phase, for a satisfactory reconstruction of the event signal, $mf > 2N + 1$ and $\eta_{\max} < (1/2N)$ should be satisfied, where $\eta_{\max}$ denotes the maximum of η_i ($\eta_{\max} = \max_i\ \eta_i$). Similar to the immobile data gathering phase, in this phase, the sink node can increase the sampling frequency f by updating it stepwise until the conditions $mf > 2N + 1$ and $\eta_{\max} < (1/2N)$ are satisfied. As soon as these conditions are satisfied, the sink node announces the last updated f as the sampling frequency of the sensor nodes. The pseudocode of this procedure is given in Algorithm 2.

Algorithm 2: Mobile Data Gathering Phase

1 **set** f as $f = (2N + 1)/m$
2 **find** $\eta_{\max} = \max_i\ \eta_i$
3 **while** $\eta_{\max} > (1/2N)$ **do**
4 $f = f + \delta$
5 **compute** $\eta_{\max}$ using the updated f
6 **end**
7 **announce** the last f is the sampling frequency

III. Performance Evaluation

Here, the performance of the sampling jitter exploitation is presented. The performance of the immobile data gathering phase is first given. Then, the mobile data gathering phase is evaluated to show the performance of the jitter exploitation. For the reconstruction of the irregularly sampled event signal, the adaptive-weight conjugate gradient method, that is a computational method for the realization of the theoretical reconstruction model introduced in Section II, is used [8]. The reconstruction error, i.e., E, is computed by $E = \|h_S^d - \widehat{h_S^d}\|/\|\widehat{h_S^d}\|$, where $\|\cdot\|$ denotes the L^2 vector norm. h_S^d is a vector including the samples of the original event signal, and $\widehat{h_S^d}$ is another vector whose elements are the samples of the reconstructed event signal. Here, data points are obtained by averaging 30 simulation runs.

A. Performance of the Immobile Data Gathering Phase

For the performance evaluation of the immobile data gathering phase, the time jitter of the sensor nodes, i.e., $\tau_i\ \forall i$, is assumed to have an upper bound denoted by $\tau_{\max}$. According to its distance to the event source location, each sensor node i has a constant jitter τ_i that is upper bounded by $\tau_{\max}$. In Fig. 2, the reconstruction error is shown with varying values of $\tau_{\max}$ for the different sampling frequency f values. For this simulation, an event signal with $N = 40$ is assumed to be sensed and sampled by $m = 5$ sensor nodes. As introduced in Section II-A for the reconstruction, $mf \geq 2N + 1 = 81$ and $\zeta_i < (1/2N) = 0.0125$ should be satisfied, where ζ_i denotes the timing gap between sample i and $i - 1$. To justify whether $\zeta_i < (1/2N)$ is satisfied in Fig. 2, in Table I, the maximum and average timing gaps, i.e., ($\zeta_{\max}$, $E[\zeta_{\max}]$, are also presented using the same simulation setting used in Fig. 2. Note that the values of $\zeta_{\max}$ and $E[\zeta_{\max}]$ are obtained from the same simulation code used in Fig. 2.

As observed in Fig. 2 and Table I, for $f = 100$, $mf = 500 > 81$ and $\zeta_{\max} < 0.0125$ are clearly satisfied, and the event signal can be successfully reconstructed with a significantly low error that is almost zero. For $f = 50$, although $mf = 250 > 81$ is satisfied, ζ_i is slightly higher than 0.0125. Therefore, the reconstruction error slightly

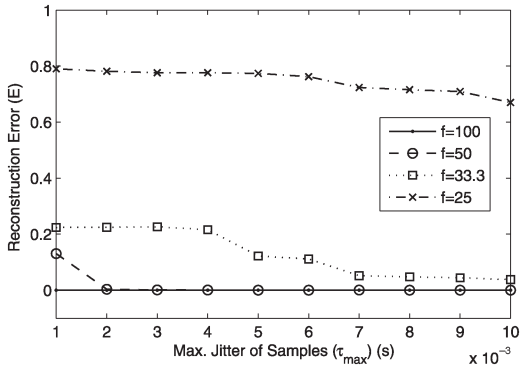

Fig. 2. Reconstruction error in the immobile data gathering phase with varying values of the maximum jitter $\tau_{\max}$.

increases for $f = 50$. On the other hand, for the cases of $f = 33.3$ and $f = 25$, $\zeta_{\max}$ is considerably higher than 0.0125. Therefore, the reconstruction error is significantly higher than the previous two cases ($f = 100$ and $f = 50$), and the event signal cannot be successfully reconstructed in these cases. Consequently, it can be easily concluded that the upper bound of the sampling jitter $\tau_{\max}$ does not directly affect the reconstruction process. Once the conditions $mf \geq 2N + 1$ and $\zeta_i < (1/2N)$ are satisfied, the event signal can be successfully reconstructed. However, the level of jitter clearly affects the timing gap ζ_i between the samples. Thus, the effect of the jitter can be considered as an indirect effect. More specifically, if the sampling jitter is high in average, this does not mean that the signal reconstruction error will be high. If the high jitter causes high timing gap levels due to the different distances of the sensors to the event source, this can result in a high error or an unsuccessful reconstruction of the event signal. In Fig. 3, the original event signal with $N = 20$ Hz, and two reconstructions of it are shown. In one reconstruction, the sampling frequency f, $\tau_{\max}$, and m are set to $f = 100$, $\tau_{\max} = 0.005$, and $m = 5$, respectively. Clearly, $mf = 500 > 2N + 1 = 41$ and $\zeta_i < (1/2 \times N) = 00.025$ are satisfied since $\zeta_{\max}$ is found as $\zeta_{\max} = 0.0066$. Therefore, the original event signal can be successfully reconstructed such that they overlap, as shown in Fig. 3. In the other reconstruction, f is reduced to $f = 20$, and for this setting, $\zeta_{\max}$ becomes 0.0467. This value is considerably higher than 0.025; therefore, the event signal cannot be reconstructed successfully. The reconstructed signal cannot follow the original event signal, as observed in Fig. 3. Consequently, these results justify the theoretical results introduced in Section II-A.

B. Performance of the Mobile Data Gathering Phase

For the performance evaluation of the mobile data gathering phase, the five vehicular sensor nodes are assumed to move around by following the ***random waypoint mobility model*** in a 2-D 50 m × 50 m environment. An event source is also assumed to be located at the coordinate (0, 0), and the event signal with $N = 20$ propagates with the speed of 50 m/s. The speed interval of the vehicular sensor nodes is set to $\{0, \omega\}$, where ω (in meters per second) denotes the upper bound of the sensor speed. The speed of each sensor node is selected from this interval for each move of sensor nodes. Therefore, ω determines the speed of the sensor nodes. The sensor speed increases as ω increases. The interval for the pause time of the sensor nodes is set to $\{0, 0.1\}$ in seconds, and the direction interval of the vehicular sensor nodes is set to $\{-180, 180\}$ in degrees. Furthermore, the walk time interval is set to $\{2, 6\}$.

In Fig. 4, the reconstruction error E is shown with varying ω for the different values of the sampling frequency f. The reconstruction error decreases with ω. This stems from the fact that sensor nodes

TABLE I
IN IMMOBILE DATA GATHERING PHASE, MAXIMUM AND AVERAGE TIMING GAPS OF SAMPLES $(\zeta_{\max}, E[\zeta_i])$, WITH VARYING VALUES OF $\tau_{\max}$ AND f

τ_{max}	0.001	0.002	0.003	0.004	0.005
$f = 100$	(0.0093,0.0019)	(0.0087,0.0019)	(0.0081,0.0019)	(0.0074,0.0020)	(0.0066,0.0020)
$f = 50$	(0.0193,0.0037)	(0.0187,0.0038)	(0.0179,0.0038)	(0.0174,0.0038)	(0.0167,0.0038)
$f = 33.3$	(0.0293,0.0054)	(0.0286,0.0054)	(0.0280,0.0054)	(0.0272,0.0055)	(0.0268,0.0055)
$f = 25$	(0.0393,0.0070)	(0.0387,0.0070)	(0.0379,0.0071)	(0.0373,0.0071)	(0.0367,0.0071)

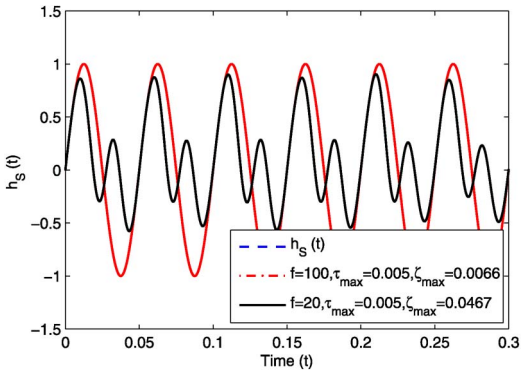

Fig. 3. In the immobile data gathering phase, reconstruction of the event signal with the changing values of f and maximum jitter $\tau_{\max}$.

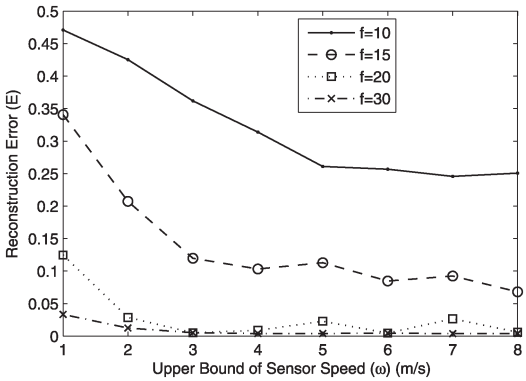

Fig. 4. Reconstruction error in the mobile data gathering phase with the varying speed interval $\{0, \omega\}$ of the vehicular sensor nodes for the different values of the sampling frequency f.

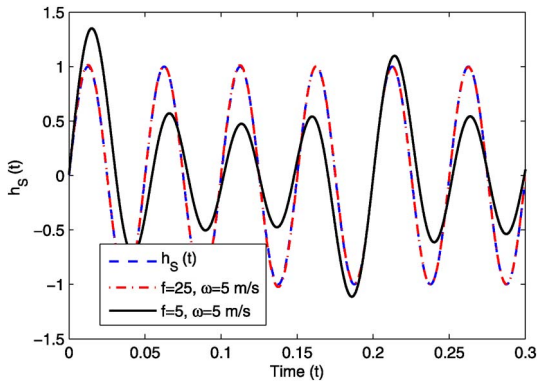

Fig. 5. In the mobile data gathering phase, the original event signal and its two reconstruction with two different values of sampling frequencies.

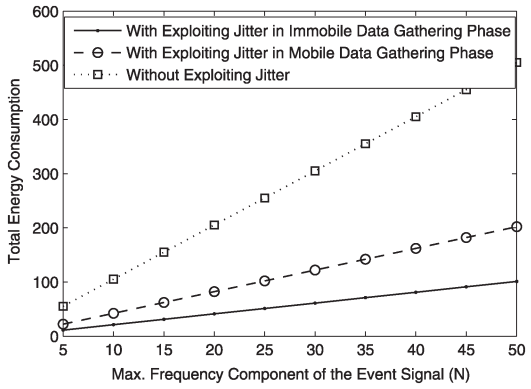

Fig. 6. Total energy consumption of sensor nodes with and without exploting sampling jitter in the mobile and immobile data gathering phase.

can be frequently close to each other as their speed increases with ω. This allows them to take samples at the time instants that are close to each other; thus, these close sampling points can satisfy the condition $\eta_i < (1/2N)$, $\forall i$, as introduced in Section II-B. In cases of $f = 25$ and $f = 20$, the event signal can be perfectly reconstructed with a low reconstruction error. However, the error rapidly grows as f is further reduced to $f = 15$ and $f = 10$. This is because, for these frequencies, the conditions $f > 2N + 1 = 41$ and $\eta_i < (1/2N)$ are no longer satisfied.

In Fig. 5, the original event signal $h_S(t)$ with $N = 20$ and two reconstructions of it are shown in the mobile data gathering phase. In one reconstruction, the sampling frequency f and the upper bound of the sensor speed ω are set to $f = 25$ and $\omega = 5$, respectively. For this setting, $mf = 125 > 2N + 1 = 41$ is clearly satisfied, and the average of the timing gaps between consecutive sampling points[3] $(\eta_i, \forall i)$ is 0.0078 such that this justifies that $\eta_i < (1/N) = 0.025$ is also satisfied. Hence, the signal is successfully reconstructed by using this setting, as observed in Fig. 5. In the other reconstruction, f is reduced to 5; thus, $mf = 25 < 2N + 1 = 41$ cannot be satisfied. Therefore, the reconstruction becomes unsuccessful, as shown in Fig. 5. In this setting, the average of the timing gaps $(\eta_i, \forall i)$ is 0.0335, and this value is considerably higher than $(1/2N) = 0.025$, i.e., $0.0335 > (1/2N) = 0.025$. Hence, this also justifies why the event signal cannot be successfully reconstructed for this setting, as observed in Fig. 5. Furthermore, through Figs. 4 and 5, it can be easily concluded that the event signal can be successfully reconstructed if the conditions $mf < 2N + 1$ and $\eta_{\max} < (1/2N)$ are satisfied regardless of the speed of the sensor nodes.

[3]The average timing gap between the consecutive sampling points is obtained by using the simulation data in Fig. 5.

C. Energy Conservation With the Sampling Jitter Exploitation

Energy consumption in VSNs increases with the sampling rate such that more packets are generated, and traffic load over the network is

amplified. Here, it is assumed that, on average, each sample of the sensor nodes consumes B units of energy to be delivered to the sink. In the immobile data gathering phase, the sensor nodes only transmit the samples of the event signal to the sink node. However, in the mobile data gathering phase, in addition to the samples, the sensor nodes also transmit their location information, i.e., $l_i\ \forall i$, as introduced in Section II-B. Here, each sensor node is assumed to consume B units of energy per sample to notify the sink node about its location update. In Fig. 6, total average energy consumption is shown for the varying values of the maximum frequency component in the event signal N with and without exploiting the sampling jitter in the immobile and mobile data gathering phases. By exploiting the sampling jitter, up to 80% and 60% energy saving in the immobile and mobile data gathering phases, respectively, can be provided for VSNs. This result clearly shows that the sampling jitter exploitation can be considered as a beneficial design tool to further improve the energy conservation performance in VSNs and WSNs.

IV. Conclusion

In this paper, it has been revealed through theoretical and numerical analyses that sampling jitter can indeed be useful for successful event signal reconstruction by selecting appropriate sampling frequency of sensor nodes according to the propagation velocity and bandwidth of the event signal. Furthermore, the given analysis can be used toward development of new adaptive energy-efficient and reliable communication techniques based on exploiting sampling jitter for improved performance in VSNs. The future research of this work includes the development of these techniques by considering the probabilistic deployments and mobility patterns of sensor nodes.

References

[1] A. V. Oppenheim, R. W. Schafer, and J. R. Buck, *Discrete-Time Signal Processing*. Upper Saddle River, NJ, USA: Prentice-Hall, 1999.

[2] M. C. Vuran, O. B. Akan, and I. F. Akyildiz, "Spatio-temporal correlation: theory and applications for wireless sensor networks," *Comput. Netw.*, vol. 45, no. 3, pp. 245–259, Jun. 2004.

[3] I. F. Akyildiz, W. Su, Y. Sankarasubramaniam, and E. Cayirci, "Wireless sensor networks: A survey," *Comput. Netw.*, vol. 38, no. 4, pp. 393–422, Mar. 2002.

[4] W. Bajwa, A. Sayeed, and R. Nowak, "Matched source-channel communication for field estimation in wireless sensor networks," in *Proc. IPSN*, Los Angeles, CA, USA, 2005, pp. 332–339.

[5] M. Gastpar and M. Vetterli, "Source-channel communication in sensor networks," in *Proc. IPSN*, Palo Alto, CA, USA, 2003, pp. 162–177.

[6] D. Ganesan, S. Ratnasamy, H. Wang, and D. Estrin, "Coping with irregular spatio-temporal sampling in sensor networks," *Comput. Commun. Rev.*, vol. 34, no. 1, pp. 125–130, Jan. 2004.

[7] A. Nordio, C.-F. Chiasserini, and E. Viterbo, "Performance of linear field reconstruction techniques with noise and uncertain sensor locations," *IEEE Trans. Signal Process.*, vol. 56, no. 8, pp. 3535–3547, Aug. 2008.

[8] H. G. Feichtinger, K. Gröchenig, and T. Strohmer, "Efficient numerical methods in non-uniform sampling theory," *Numer. Math.*, vol. 69, no. 4, pp. 423–440, Feb. 1995.

[9] J. C. Chen, "Source localization and beamforming," *IEEE Commun. Mag.*, vol. 19, no. 2, pp. 30–39, Mar. 2002.

[10] K. Langendoen and N. Reijers, "Distributed localization in wireless sensor networks: A quantitative comparison," *Comput. Netw.*, vol. 43, no. 4, pp. 499–518, Nov. 2003.

Wireless Energy and Information Transfer Tradeoff for Limited-Feedback Multiantenna Systems With Energy Beamforming

Xiaoming Chen, Chau Yuen, and Zhaoyang Zhang

***Abstract*—In this paper, we consider a multiantenna system where the receiver should harvest energy from the transmitter by wireless energy transfer to support its wireless information transmission. To maximize the harvesting energy, we propose the performance of adaptive *energy beamforming* according to the instantaneous channel state information (CSI). To help the transmitter obtain the CSI for energy beamforming, we further propose a win-win CSI quantization feedback strategy to improve the efficiencies of both power and information transmission. The focus of this paper is on the tradeoff of wireless energy and information transfer by adjusting the transfer duration with a total duration constraint. By revealing the relationship between transmit power, transfer duration, and feedback amount, we derive two wireless energy and information transfer tradeoff schemes by maximizing an upper bound and an approximate lower bound of the average information transmission rate, respectively. Moreover, the impact of imperfect CSI at the receiver is investigated, and the corresponding wireless energy and information transfer tradeoff scheme is also given. Finally, numerical results validate the effectiveness of the proposed schemes.**

***Index Terms*—Energy beamforming, limited feedback, resource allocation, wireless energy and information transfer.**

I. Introduction

Recently, wireless energy transfer has aroused the general interest of the wireless research community, as it can effectively prolong the lifetime of the power-limited node or network in a relatively simple way [1]–[3]. As a typical example, in the medical area, equipment implanted in the body can be powered through wireless power transfer [4].

In general, wireless energy transfer from a power source to a receiver is implemented through electromagnetic propagation [5]. Since electronic energy is isotropically propagated if the transmit antenna is isotropic, the receiver only harvests a portion of the transmitted energy without specific control, resulting in a low energy transfer efficiency. To maximize the harvested energy, it is necessary to coordinate transmit direction to the receiver, namely, energy beamforming. The key to energy beamforming is the achievement of channel state information

Manuscript received August 20, 2012; revised November 28, 2012, March 3, 2013, and May 7, 2013; accepted July 23, 2013. Date of publication July 25, 2013; date of current version January 13, 2014. This work was supported in part by the Natural Science Foundation Program of China under Grant 61300195, by the Natural Science Foundation Program of Jiangsu Province under Grant 2013001012, by the Open Research Fund of the State Key Laboratory of Integrated Service Networks of Xidian University under Grant ISN14-01, by the Doctoral Fund of the Ministry of Education of China under Grant 20123218120022, and by the Singapore University of Technology and Design under Grant SUTD-ZJU/RES/02/2011. The review of this paper was coordinated by Dr. S. Tomasin.

X. Chen is with the College of Electronic and Information Engineering, Nanjing University of Aeronautics and Astronautics, 210016 Nanjing, China, and also with the State Key Laboratory of Integrated Service Networks, Xidian University, Xi'an 710126, China (e-mail: chenxiaoming@nuaa.edu.cn).

C. Yuen is with the Singapore University of Technology and Design, Singapore 138682 (e-mail: yuenchau@sutd.edu.sg).

Z. Zhang is with the Department of Information Science and Electronic Engineering, Zhejiang University, Hangzhou 310027, China (e-mail: ning_ming@zju.edu.cn).

Color versions of one or more of the figures in this paper are available online at http://ieeexplore.ieee.org.

Digital Object Identifier 10.1109/TVT.2013.2274800